



## Coupling phenomenological model of expansion with mechanical model of starchy products extrusion

Magdalena Kristiawan, Guy Della Valle, Kamal Kansou, Amadou Ndiaye,  
Bruno Vergnes, Chantal David

### ► To cite this version:

Magdalena Kristiawan, Guy Della Valle, Kamal Kansou, Amadou Ndiaye, Bruno Vergnes, et al.. Coupling phenomenological model of expansion with mechanical model of starchy products extrusion. 49. congrès du Groupe Français de Rhéologie: Rhéologie et approches mul physiques couplées, Groupe Français de Rhéologie (GFR). Paris, FRA., Oct 2014, Grenoble, France. hal-01190146

**HAL Id: hal-01190146**

**<https://hal.science/hal-01190146>**

Submitted on 1 Sep 2015

**HAL** is a multi-disciplinary open access archive for the deposit and dissemination of scientific research documents, whether they are published or not. The documents may come from teaching and research institutions in France or abroad, or from public or private research centers.

L'archive ouverte pluridisciplinaire **HAL**, est destinée au dépôt et à la diffusion de documents scientifiques de niveau recherche, publiés ou non, émanant des établissements d'enseignement et de recherche français ou étrangers, des laboratoires publics ou privés.

# A phenomenological model of starch expansion by extrusion

<sup>1</sup>M. Kristiawan, <sup>1</sup>G. Della Valle, <sup>1</sup>K. Kansou, <sup>2</sup>A. Ndiaye, <sup>3</sup>B. Vergnes and <sup>4</sup>C. David

<sup>1</sup>INRA, UR 1268 Biopolymers Interactions and Assemblies (BIA), BP 71627, 44316 Nantes, France

<sup>2</sup>INRA, USC 1368 Institut de Mécanique et d'Ingénierie (I2M), UMR 5295 CNRS, Univ. Bordeaux 1, 33405 Talence Cedex, France

<sup>3</sup>MINES ParisTech, CEMEF, UMR CNRS 7635, BP 207, 06904 Sophia-Antipolis Cedex, France

<sup>4</sup>Sciences Computers Consultants, 10 rue du Plateau des Glières F-42000 Saint-Etienne, France

Contact person : [magdalena.kristiawan@nantes.inra.fr](mailto:magdalena.kristiawan@nantes.inra.fr)

**Abstract** : During extrusion of starchy products, the molten material is forced through a die so that the sudden pressure drop causes part of the water to vaporize giving an expanded, cellular structure. The objective of this work was to elaborate a phenomenological model of expansion and coupled it with Ludovic<sup>®</sup> mechanistic model of twin screw extrusion process. From experimental results that cover a wide range of thermomechanical conditions, a conceptual map of influence relationships between input and output variables was built. It took into account the phenomena of bubbles nucleation, growth, coalescence, shrinkage and setting, in a viscoelastic medium. The input variables were the moisture content  $MC$ ; melt temperature  $T_p$ , specific mechanical energy  $SME$ , shear viscosity  $\eta$  at the die exit, computed by Ludovic<sup>®</sup>, and the material storage moduli  $E'(T_p > T_g)$ . The outputs of the model were the macrostructure (volumetric expansion index  $VEI$ , anisotropy) and cellular structure (fineness) of solid foams. Then a general model was suggested:  $VEI = \alpha (\eta/\eta_0)^n$  in which  $\alpha$  and  $n$  depend on  $T_p$ ,  $MC$ ,  $SME$  and  $E'$  and the link between anisotropy and fineness was established.

**Keywords** : amylose, cellular structure, expansion indices, shear viscosity, elongational viscosity.

[Abridged French version on last page]

## 1. Introduction

Extrusion is extensively used for production of different categories of starch based foods. After melting, the viscous material is forced through a die where a part of superheated water evaporates due to the sudden pressure drop. The vapor blows the material to an expanded, porous structure. The product cools down due to the evaporation and convective heat transfer and, crossing the glass transition, it becomes solid. The expansion at the die exit is thus a very complex process involving a succession of dynamic phenomena, occurring in a short time interval (less than 1 s), such as bubble nucleation and growth, coalescence, shrinkage and finally setting when the melt matrix becomes glassy. Hence, extruded products can have same density but different cellular architectures depending on the raw material formulation and processing parameters [1, 2]. Both features in-turn impact the texture, nutritional and sensory attributes of the product.

The growth of a bubble was modelled mechanically using a “cell model” [3] in which the gas bubble is surrounded by an envelope of liquid (with finite thickness), providing a finite amount of liquid for

expansion and thus limiting the final radius of the bubble. The expansion rate depends on the pressure difference across the shell of bubbles and on the rheological properties of starch melt (shear viscosity). This model presents two important features: depletion of dissolved gas and progressively thinning bubble walls. Thereafter, other models followed a similar approach and the main differences between them can be classified according to the assumptions made [4 - 11]: presence of heat transfer, dependence of physical parameters (shear viscosity, diffusion coefficient) on temperature and moisture content, coupling microscopic bubble growth model (on bubble scale) with macroscopic mass, momentum and heat transfer (on the extrudate scale) and rheological model for the melt. Different forms of the equation of motion linking the bubble radius with the pressure in the bubble can be distinguished by taking into account or not the surface tension effects, elastic effects, yield stress and inertial terms.

Most authors modelled the expansion as the sequence of bubble growth and shrinkage phenomena only and did not take into account the nucleation and coalescence. They also often took an

initial bubble number as parameter, and all neglected the role of elongational viscosity. Pai et al. [12] suggested that the extrudate expansion depends on the interplay of shear and extensional viscosities. So these numerical mechanistic models are not complete, but they are also too complex to be coupled with present software for simulation of co-rotating twin-screw extrusion process (Ludovic®) [13]; so there is a need for simpler model in order to extend the capability of this software to predict the cellular structure of starchy extruded foams.

The objective of this work was to elaborate a phenomenological model of expansion in function of processing variables and melt rheology and thereafter to couple it with Ludovic® mechanistic model. Qualitative representation, using concept map, was used to reason about the physical process of vapor expansion, in order to improve our understanding and to suggest a mathematical expression of the phenomenological models. The melt rheology involved shear and elongational viscosities. The input variables such as melt temperature  $T_p$ , specific mechanical energy  $SME$  and shear viscosity  $\eta$  can be computed by Ludovic®. The other inputs were moisture content  $MC$  and die geometry. The output variables were the foam macrostructure, described by anisotropy ( $AF$ ) and bulk expansion indices ( $VEI$  and  $SEI$ ) deduced from density, and cellular microstructure assessed by fineness ( $F$ ), computed from mean cell size and mean cell wall thickness.

## 2. Materials and method

### 2.1 Materials and extrusion

Table 1. Raw material

Starch	Product	Amylose / Amylopectine
A	Amylomaize	70 / 30
B	Blend A : D = 2 : 1	47 / 53
C	Blend A : D = 1 : 2	23.5 / 76.5
D	Waxy maize	0 / 99

The modeling work was realized on the published data of maize starches expansion using a twin-screw extruder Clextral BC-45 equipped with a slit die rheometer (Rheopac) [1, 14, 15]. The maize starches with different amylose content were used to study the influence of elongational viscosity (Table 1). The overview of extrusion variables is shown in Table 2. As a general rule, low moisture content led to medium or high  $SME$  and  $T_p$  whereas high moisture content gave low or medium  $SME$  and  $T_p$ . Extruder configurations and sets of operating

conditions have been fully detailed formerly [14]. For each experimental set (combination of amylose content,  $MC$ ,  $T_p$ ,  $SME$ , die height), the shear rate in the Rheopac channels was varied between 10 and 200  $s^{-1}$ , and the melt shear viscosity has been determined from pressure drop in channel 1, after Rabinowitsch corrections. The extruded ribbon was collected from channel 1 for structural characterization after drying and conditioning to a moisture content about 0.1 (dry basis).

Table 2. Operating variables at the die exit

Control variables	$MC$	$T$ °C	$SME$ kWh.t <sup>-1</sup>	$\eta$ Pa.s	Die height* $h_d$ (mm)	Entrance opening** $h$ (mm)
Min	0.21	105	101	80	3	0.3
Max	0.36	186	580	1200	2	3

\*Rheopac main channel height

\*\*Orifice opening of the entrance of the channel 1

### 2.2 Structural characterization

#### 2.2.1 Macrostructure

The bulk expansion indices,  $VEI$  for volumetric,  $SEI$  for radial and  $LEI$  for longitudinal expansion, were defined according to the definitions given by Alvarez-Martinez et al. [16]. Longitudinal means the expansion in extruder die flow direction and radial in the orthogonal plane.

$$VEI = \frac{\rho_m(1 - MC_m)}{\rho_e(1 - MC_e)} \quad (1)$$

$$SEI = \frac{S_e}{S_d} \quad (2)$$

$$LEI = S_d \cdot L_{se} \cdot \rho_m \frac{1 - MC_m}{1 - MC_e} \quad (3)$$

Finally,  $VEI$  can be defined as

$$VEI = LEI \times SEI \quad (4)$$

where  $\rho$  is the density ( $kg.m^{-3}$ ),  $MC$  is the moisture content (fraction on total wet basis),  $S$  is the cross section ( $m^2$ ) and  $L_{se}$  is the specific length of extrudate ( $m.kg^{-1}$ ). Subscripts  $d$ ,  $e$  and  $m$  refer to die, extrudate and melt, respectively.

It holds for isotropic expansion:  $LEI = SEI^{0.5}$  [2]. The anisotropy factor ( $AF$ ) was defined as:

$$AF = \frac{LEI}{SEI^{0.5}} = \frac{VEI}{SEI^{3/2}} \quad (5)$$

If  $AF$  is greater than 1, the longitudinal expansion prevails the radial expansion and vice versa.

#### 2.2.2 Cellular structure

The mean cell size ( $MCS$  in mm) and mean cell wall thickness ( $MWT$  in  $\mu\text{m}$ ) of extruded starch foams were determined from the volumetric distributions of cells and cell walls after analyses of 3D images acquired by X-ray tomography by Babin et al. [1]. Then we defined the fineness ( $F$ ) of the microstructure:

$$F = \sqrt{\frac{\left(\frac{1}{MCS}\right)^2 + \left(\frac{250}{MWT}\right)^2}{2}} \quad (6)$$

where 1 mm and 250  $\mu\text{m}$  are average values encountered for  $MCS$  and  $MCWT$ , respectively [1, 2]. Then  $F > 1$  means extrudate has a fine cellular structure and  $F < 1$  a coarse one.

### 2.3. Modelling approach

Because of the complexity of expansion phenomena, the first stage involved the knowledge reasoning approach: (a) collecting scientific knowledge from literature, expertise and experimental data, (b) representing knowledge with concept map. Using the concept map (influence graph), the direction and magnitude of influence relationships between input variables and expansion phenomena and output variables were determined. Then the net effect of input variables on one output variable was deduced.

In the second stage, the phenomenological models for volumetric ( $VEI$ ) and radial ( $SEI$ ) expansion indices were established using variables defined in the previous step and literature data [1, 14, 15]. The anisotropy factor ( $AF$ ) was computed from  $VEI$  and  $SEI$  models and compared to experimental data, using Eq. 5. The cell fineness ( $F$ ) was finally related to  $AF$ .

The validity of Ludovic<sup>®</sup> simulation results for flow variables in an extruder was also verified. For the molten maize starches (with amylose content of 0 and 0.23), the constants ( $K$  and  $n$ ) of power law model for shear viscosity  $\eta$  were expressed according to [14]:

$$\eta = K\dot{\gamma}^{n-1} \quad (7)$$

$$K = K_0 \exp\left[\frac{E}{R T_a} - \alpha MC - \beta SME\right] \quad (8)$$

$$m = m_0 + \alpha_1 T + \alpha_2 MC + \alpha_3 SME + \alpha_4 T \cdot MC + \alpha_5 T \cdot SME + \alpha_6 MCSME \quad (9)$$

Then the SME - shear viscosity coupling mode was activated in the Ludovic<sup>®</sup> input for material rheological model. The shear viscosity at the die exit was also calculated using Ludovic<sup>®</sup>.

### 2.4. Least square fit of model and statistical analysis

Data regression was done using non-linear least square (NLLS) method by Microsoft Excel Solver. Then the statistical analysis was done using SOLVERSTAT, in Microsoft Excel that yields the statistical regression diagnostics after LS fitting by Solver [17].

The models must pass following checks for regression analysis: (1) Examination of model quality with a  $F$ -Test. If  $F_{\text{calc.}} > F_{\text{crit.}}$  then the regression is significant. (2) Examination of regression method quality using *Levene*  $F$ -Test to check that residuals have constant variance (if  $F_{\text{calc.}} < F_{\text{crit.}}$  is fulfilled). (3) Examination of significance model parameters with a Student  $t$ -Test that checks if the single parameter is statistically different from zero (if  $t_{\text{cal.}} > t_{\text{crit.}}$  is fulfilled). (4) Examination of goodness model fit using several statistical criterias: high value of Coefficient of Multiple Determination  $R^2$ , Adjusted Coefficient of Multiple Determination  $R^2_{\text{adj.}}$  and low value of Root Mean Squared Error  $RMSE$ . After discarding non-significant model parameters, the NLLS fitting and SOLVERSTAT were re-launched for reduced  $VEI$  and  $SEI$  models.

NLLS fit for  $VEI$  and  $SEI$  with objective of minimizing its  $SSE$  has first given high  $R^2$  values, 0.93 and 0.85 (results not shown). Then anisotropy factor ( $AF$ ) computed from these  $VEI$  and  $SEI$  models, according to Eq. 5, did not fit the experimental data ( $R^2 = 0.17$ ). Thus, we used an optimization strategy to obtain similar values for  $R^2$  of  $VEI$ ,  $SEI$  and  $AF$  by minimizing the weighted sum of  $SSE$  of  $AF$ ,  $SEI$  and  $VEI$  in NLLS fit:

$$SSE_{\text{opt}} = SSE_{AF} + w_1 SSE_{SEI} + w_2 SSE_{VEI} \quad (10)$$

where weight  $w_1 = 0.3$  and weight  $w_2 = 0.05$

By the means of the weight  $w_1$  and  $w_2$  we changed the  $R^2$  of  $AF$ ,  $SEI$  and  $VEI$  simultaneously.

The weight  $w_1 = 0.3$  and  $w_2 = 0.05$  were chosen by trial and error method which assured a high value of  $R^2$  for  $AF$  (0.78) keeping the both  $R^2$  for  $SEI$  (0.77) and for  $VEI$  (0.88) high enough, see Tables 3 and 4.

## 3. Results and discussion

### 3.1 Qualitative reasoning of vapor expansion

The concept map defined relations between input variables (temperature of product in die exit  $T_p$ , moisture content  $MC$ , shear viscosity  $\eta(\dot{\gamma})$ , storage modulus  $E'(T_g)$ , expansion phenomena (nucleation, bubble growth, coalescence, shrinkage, setting) and

output variables (foam density, anisotropy factor). These relations are qualitative; they are expressed by the signs + or -. The sign + signifies positive effect and the sign - stands for negative effect. The magnitude of the effect is quantified with a number of signs. The net effect of one input variable on one output variable is the sum of all effects between these variables.

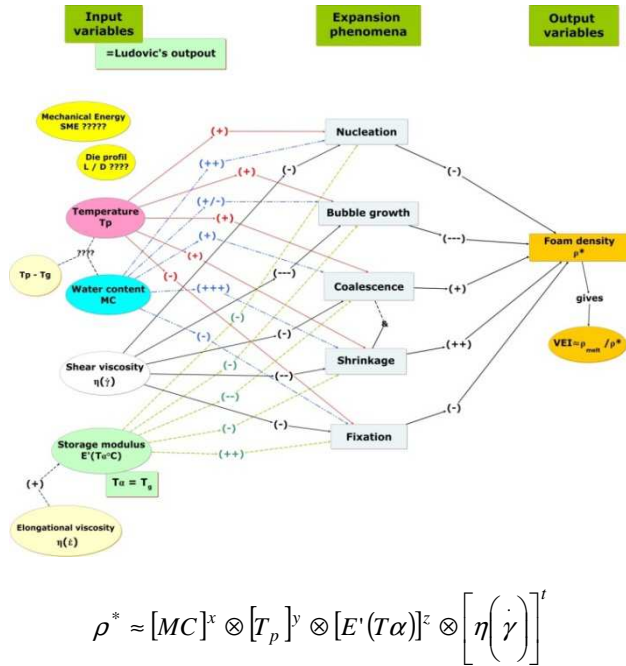


Fig. 1. Concept map of phenomenological model of expansion

At present, the data of elongational viscosity of starchy products is scarce in literature due to technical difficulties in measurements. Because this variable also reflects elastic property [1], we assumed that the storage modulus  $E'$  ( $T > T_g$ ) could replace the elongational viscosity in the model (Fig. 1).

### 3.2 Validation of Ludovic® simulation

A good agreement between the computed and measured melt temperature at the die exit was found (data not shown). Although a good correlation between computed and measured  $SME$  was obtained ( $R^2 = 0.8 - 0.9$ ), the computed total dissipated energy (total  $SME$ ) was generally underestimated (Fig. 2), likely because Ludovic® model takes into account only the viscous dissipation after melting section and neglects mechanical energy delivered to the product for melting, solid friction and conveying. The computed pressure at the die entrance was also underestimated and the correlation between the measured and the computed pressure was poor ( $R^2 < 0.50$ ) (data not shown). It could be improved by taking more accurately die geometry into account.

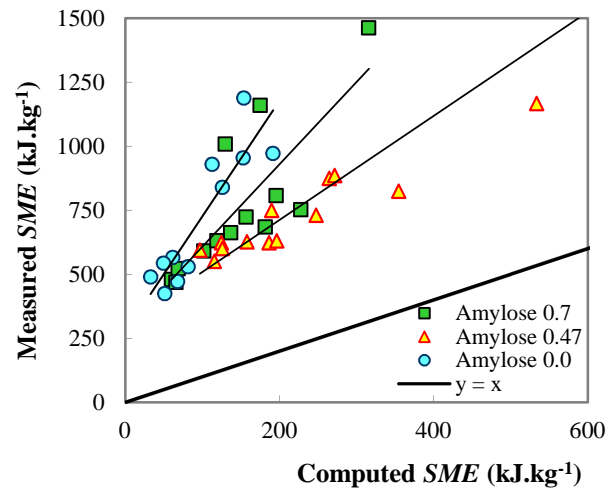


Fig. 2. Validation of Ludovic® simulation

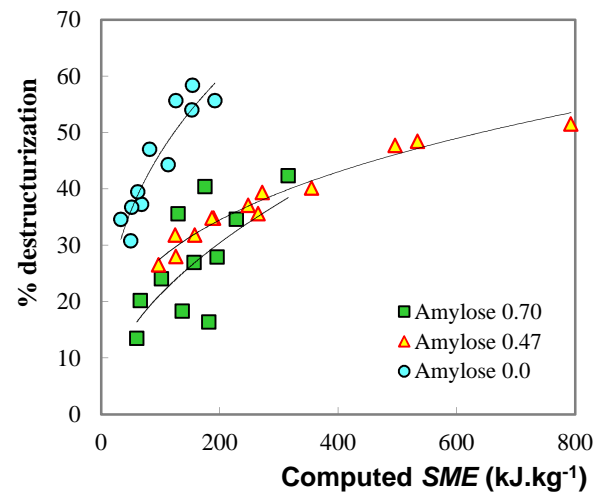


Fig. 3. Variations of starch destructurezation with  $SME$

The computed  $SME$  was useful to predict starch destructurezation by extrusion process (Fig. 3). The starch destructurezation was quantified by decrease of material intrinsic viscosity ( $\text{ml.g}^{-1}$ ) after extrusion. The good correlation between starch destructurezation (%) and  $SME$  ( $R^2 = 0.85 - 0.95$ ) was obtained for starch with amylose contents of 0.47 and 0.0, on the other hand, a poor correlation ( $R^2 = 0.47$ ) was found for amylose content of 0.7 (Fig. 3). The amylopectine with high molecular weight ( $M_w \approx 10^8 \text{ kg.mol}^{-1}$ ) was found more sensitive to thermomechanical treatment than amylose of lower molecular weight ( $M_w \approx 10^6 \text{ kg.mol}^{-1}$ ).

In conclusion, the Ludovic® simulation was reliable to compute the flow variables at the die exit, that can be used, in turn, as the input variables for expansion phenomenological model.

### 3.3 Phenomenological model of expansion

As shown by experimental results in Fig. 4, the expansion index  $VEI$  decreased with shear viscosity following a power-law trend.  $VEI$  also decreased with increasing moisture content at constant shear viscosity and close to melt temperature [15]. The same tendency was found for temperature effect on constant moisture content.  $SEI$  followed the same trend as  $VEI$ . These results illustrated the direct effect of shear viscosity, moisture content and temperature on expansion, as shown in the concept map (Fig. 1).

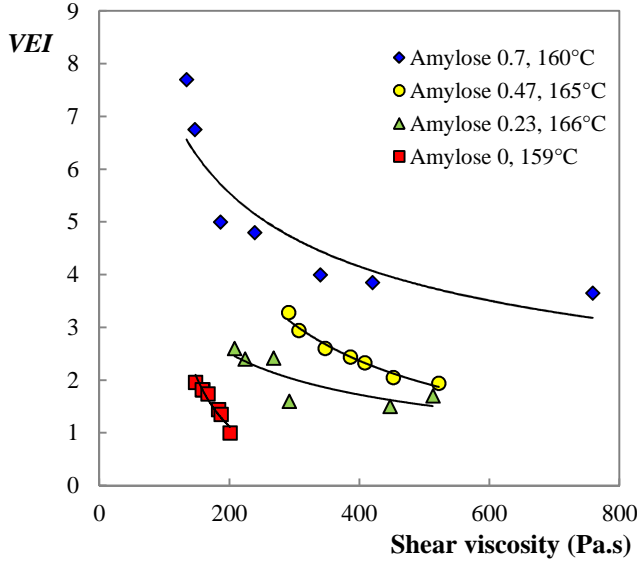


Fig. 4. Variation of volumetric expansion index ( $VEI$ ) with melt shear viscosity for different amylose content ( $MC = 0.245$ ,  $T_p = 160-165$  °C,  $200 < SME < 250$  kWh/t).

As this trend was observed for most extrusion conditions, and following the concept map (Fig. 1), we proposed to model expansion indices with power type functions:

$$VEI = \alpha_v \left( \frac{\eta}{\eta_0} \right)^{n_v} \text{ and } SEI = \alpha_s \left( \frac{\eta}{\eta_0} \right)^{n_s} \quad (11a,b)$$

and the effect of the processing variables on both  $\alpha_i$  and  $n_i$  by:

$$\alpha_i = b_0 (MC/MC_0)^{b_1} (T_p/T_0)^{b_2} (SME/SME_0)^{b_3} (E'/E_0)^{b_4} (h/h_d)^{b_5} \quad (12)$$

$$n_i = b_6 (MC/MC_0)^{b_7} (T_p/T_0)^{b_8} (SME/SME_0)^{b_9} (E'/E_0)^{b_{10}} (h/h_d)^{b_{11}} \quad (13)$$

The processing variables with subscript 0 were used with the aim to obtain dimensionless values.  $h_d$  is the height of slit die (or the height of the channel 1 of Rheopac);  $h$  is the orifice opening of the entrance of the channel 1.  $E'$  is the storage modulus at glass transition temperature. The variation of  $E'$  with

amylose and moisture content can be estimated from literature [20]. The same reference for processing variables was used for modeling  $VEI$  and  $SEI$ :  $MC_0 = 0.205$ ,  $T_0 = 160$ °C,  $SME_0 = 200$  kWh/t,  $\eta_0 = 1000$  Pa.s,  $E'_0 = 485$  MPa.

Table 3. Results of statistical analysis for  $VEI$  model

Statistic result		$F_{crit.}$	
$F$ value for Levene Test		1.543	3.866
$F$ value for $F$ -Test		251.1	1.815
$R^2$		0.8833	
$R^2$ adj		0.8798	
$RMSE$		0.2531	
Model parameters		Standard error	$t_{calc.}^*$
$b_0$	9.87	0.160	17.7
$b_1$	-4.71	0.162	29.1
$b_2$	-1.71	0.209	8.2
$b_3$	n.s.		
$b_4$	0.37	0.017	22.4
$b_5$	0.21	0.025	8.2
$b_6$	-0.15	0.03	5
$b_7$	1.23	0.363	3.4
$b_8$	-1.92	0.475	4
$b_9$	-1.48	0.236	6.3
$b_{10}$	n.s.		
$b_{11}$	-0.4	0.062	6.4

Significance level 0.05

\* $t_{crit} = 1.967$

n.s. = not significant

12 parameters may appear as a heavy set for the model, but it was supported by the large number of experimental data (about 400) leading to a large  $dof$  value and a low  $F$  value, as shown from the results of statistical analysis at significance level of 0.05 (Tables 3 and 4). They allowed to consider not only the  $R^2$  but also the adjusted  $R^2$ , which reflected the robustness of the model, whereas the  $t$  value of Student Test, computed for each parameter expressed its significance at 0.05.

The term  $h/h_d$  may represent the deformation history in the slit die. If this term was neglected, the model fitted poorly the experimental data,  $R^2 = 0.65$  and 0.47, for  $VEI$  and  $SEI$ , respectively. Alvarez-Martinez et al. [16] incorporated the term of total strain in the die into their general expansion model, and suggested it characterized the effect of alignment of amylose/amylopectine chains and elastic energy storage of the melt.

Table 4. Results of statistical analysis for  $SEI$  model

Statistic result		$F_{crit.}$	
$F$ value for Levene Test		1.052	3.866
$F$ value for $F$ -Test		113.2	1.815
$R^2$		0.7733	
$R^2$ adj		0.7665	
$RMSE$		0.2844	
Model parameters		Standard error	$t_{calc.}^*$
$b_0$	5.09	0.203	14.33
$b_1$	-4.6	0.206	22.32
$b_2$	-2.74	0.213	12.87
$b_3$	-0.25	0.052	4.8
$b_4$	n.s.		
$b_5$	0.46	0.028	16.28
$b_6$	-0.076	0.036	2.13
$b_7$	4.92	1.369	3.59
$b_8$	n.s.		
$b_9$	n.s.		
$b_{10}$	0.9	0.302	2.98
$b_{11}$	-0.88	0.175	5.04

Significance level 0.05

\* $t_{crit} = 1.967$ 

n.s. = not significant

Della Valle et al. [15] pointed out the important role of  $T_g$  which evolves in function of moisture content (evaporation) during expansion. They supposed that the product structure is fixed during expansion at a temperature  $30^\circ\text{C}$  higher than  $T_g$ . We did not consider the effect of  $(T_p - T_g)$  at the die exit in our models because the difference in  $T_g$  between the four starches can be neglected.

The predicted effect of amylose content on  $VEI$  in function of shear viscosity is shown in Fig. 5. The predicted results were compared to measured ones. Fig. 5 showed that the estimated storage moduli ( $E'(T_g)$ ) was capable to represent the role of amylose content, thus, the elongational viscosity, as one of model parameters. Using approximate  $E'(T_g)$ , the models, Eqs. 11-13, were able to predict correctly the behavior of macrostructure in function of amylose content. At the same shear viscosity, the predicted  $VEI$  increased with amylose content (with elongational viscosity) for moisture content 0.245 and  $T_p$  159-165°C

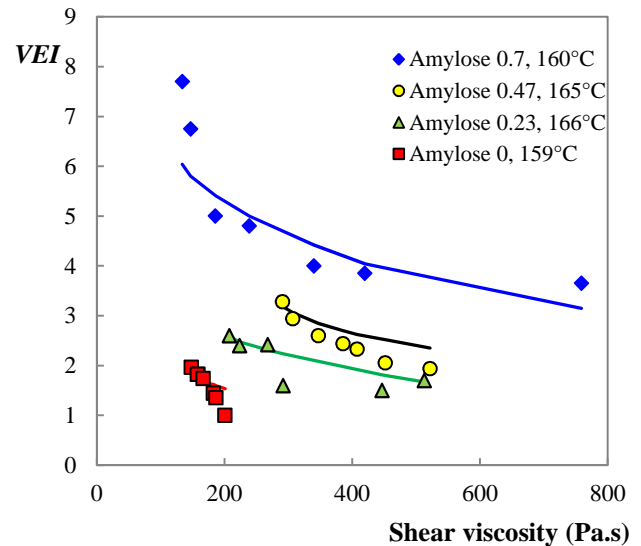


Fig. 5. Experiment vs simulation. Effect of amylose content on  $VEI$  at  $150 < SME < 250 \text{ kWh.t}^{-1}$ . Symbols represent measured value. Lines represent predicted values using model.

### 3.4 Relation between macrostructure and cellular structure

We established the mapping of anisotropy and corresponding cellular structure (Fig. 6) using literature data [1]. The anisotropy was presented by the variation of longitudinal expansion index  $LEI$  with square root of radial expansion index  $SEI$ . There is a general trend of  $LEI$  to be correlated negatively with  $SEI$ , which is marked by iso-density curves.  $LEI$  increases with amylose content whereas  $SEI$  increases with amylopectin content.

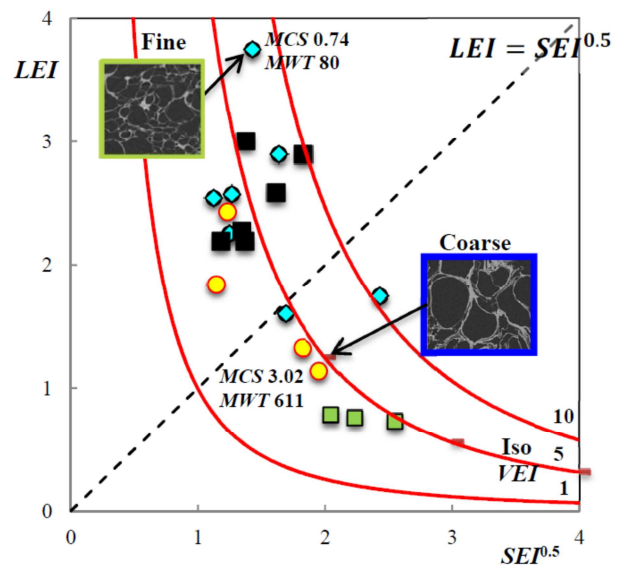


Fig. 6. Mapping of anisotropy and cellular structure. Amylose content:  $\blacklozenge$  0.7 ;  $\blacksquare$  0.47;  $\bullet$  0.25;  $\blacksquare$  0



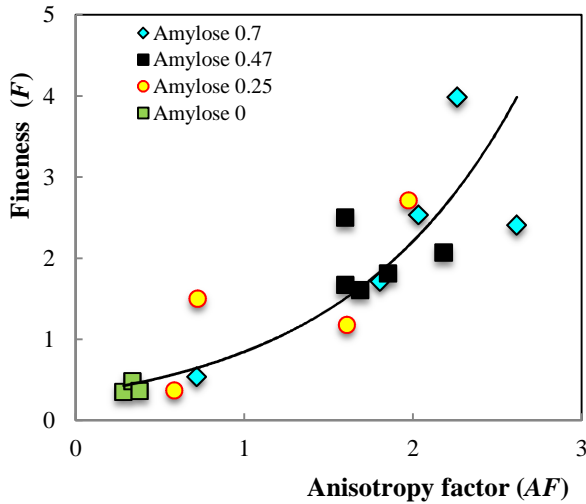


Fig. 7. Scaling down from macroscopic structure (anisotropy factor) to microscopic structure (cell fineness)

From Figs. 6 and 7, the higher amylose content, the higher was anisotropy factor obtained with favored longitudinal expansion ( $LEI \gg SEI^{0.5}$ ). On the other hand, radial expansion was more favored at higher amylopectin content ( $LEI \ll SEI^{0.5}$ ). Extruded foams with favored longitudinal expansion were characterized by finer cells and thinner cell wall than those for which radial expansion was favored, characterized by coarser cells and thicker cell wall.

The higher elongational viscosity could reduce the coalescence during bubble expansion, which may explain why amylose would attribute higher  $VEI$  even though the shear viscosity of starch rises with amylose content. This balance could be assessed by determining Trouton number. According to [16], the molecular structure could play a role in controlling anisotropy of expansion. The aligned straight chain of amylose would be more difficult to pull apart, thus to swell at the die exit, than the aligned amylopectin that contains many side-branches, so the  $SEI$  would be lower for starch with important amylose content. The high ratio  $L/D$  of the die also strengthens this effect.

Finally, there was a good fit ( $R^2 = 0.82$ ) between cell fineness ( $F$ ) and anisotropy factor ( $AF$ ) computed from experimental data of  $MCS$ ,  $MWT$ ,  $VEI$  and  $SEI$  [1] (Fig. 7):

$$F = 0.32 \exp(0.96 AF) \quad (14)$$

This result showed that the computed  $AF$  from  $VEI$  and  $SEI$  models can be used to predict cellular fineness quantitatively using Eq. 14.

## 4. Conclusion

By reasoning qualitatively from literature and expertise, we have built a concept map which provides a good understanding of the effect of material properties and processing variables on vapor expansion phenomena during extrusion.

Consequently, power law models of bulk expansion indices have been determined with good fit and satisfactory prediction capacity, involving rheological properties, elongational viscosity being represented by material storage moduli  $E'$  ( $T > T_g$ ). Die geometry, likely reflecting the melt deformation history in the die, cannot be neglected. Scale down from macroscopic expansion indices to cellular structural features could be achieved since the cell fineness was modeled as a function of computed anisotropy factor.

These models will now be validated with experimental data from literature, reflecting different operating conditions and materials, for example extrusion of whole wheat flour [2, 18, 19], for which rheological properties are available. This approach can also involve the glass transition temperature  $T_g$  which reflects the effect on expansion of more complex formulation (addition of sugar, salt, fiber, etc. in the feed).

Then the models could be integrated into the interface of Ludovic® in order to predict macro- and cellular structures of starchy foams.

## References

- [1] Babin, P., Della Valle, G., Dendievel, R., Lourdin, D., Salvo, L. *Carbohydr. Polym.*, 68(2), 329-340 (2007).
- [2] Robin, F., Engmann, J., Pineau, N., Chanvrier, H., Bovet, N., Della Valle, G. *J. Food Eng.*, 98(1), 19-27 (2010).
- [3] Amon, M., Denson, C.D. *Polym. Eng. Sci.*, 24(13), 1026-1034 (1984).
- [4] Arefmanesh, A., Advani, S.G., Michaelides, E.E. *Int. J. Heat Mass Tran.*, 35(7), 1711-1722 (1992).
- [5] Fan, J., Mitchell, J.R., Blanshard, J.M.V. *J. Food Eng.*, 23(3), 337-356 (1994).
- [6] Arefmanesh, A., Advani, S.G. *Polym. Eng. Sci.*, 35(3), 252-260 (1995).
- [7] Schwartzberg, H.G., Wu, J.P.C., Nussinovitch, A., Mugerwa, J. *J. Food Eng.*, 25(3), 329-372 (1995).
- [8] Ramesh, N.S., Malwitz, N. *J. Cell. Plast.*, 35(3), 199-209 (1999).
- [9] Shimoda, M., Tsujimura, I., Tanigaki, M., Ohshima, M. *J. Cell. Plast.*, 37(6), 517-536 (2001).
- [10] Alavi, S.H., Rizvi, S.S.H., Harriott, P. *Food Res. Int.*, 36(4), 309-319 (2003).



- [11] Wang, L., Ganjyal, G., Jones, D.D., Weller, C.L., Hanna, M.A. *Adv. Polym. Tech.*, 24(1), 29-45 (2005).
- [12] Pai, D.A., Blake, O.A., Hamaker, B.R., & Campanella, O.H. *J. Cereal Sci.*, 50(2), 227-234 (2009).
- [13] Berzin, F., Tara, A., Tighzert, L., Vergnes, B. *Polym. Eng. Sci.*, 50(9), 1758-1766 (2010).
- [14] Della Valle, G., Colonna, P., Patria, A. *J. Rheol.*, 40, 347-362 (1996).
- [15] Della Valle, G., Vergnes, B., Colonna, P., Patria, A. *J. Food Eng.*, 31(3), 277-295 (1997).
- [16] Alvarez-Martinez, A., Kondury, K.P., Harper, J.M. (1988). *J. Food Sci.*, 53(2), 609-615 (1988).
- [17] Comuzzi, C., Polese, P., Melchior, A., Portanova, R., Tolazzi, M. *Talanta*, 59(1), 67-80 (2003).
- [18] Robin, F., Dubois, C., Pineau, N., Labat, E., Théoduloz, C., Curti, D. *J. Cereal Sci.*, 56(2), 358-366 (2012).
- [19] Robin, F., Dattinger, S., Boire, A., Forny, L., Horvat, M., Schuchmann, H.P., Palzer, S. *J. Food Eng.*, 109(3), 414-423 (2012).
- [20] Ditudompo, S., Takhar, P.S., Ganjyal, G.M., Hanna, M.A. *J. Texture Stud.*, 44(3), 225-237 (2013).

### [Abridged French version]

Dans le procédé de cuisson-extrusion des produits amylacés, la matière fondue est forcée à travers une filière. La détente instantanée à la sortie de la filière entraîne l'auto-vaporisation de l'eau, donc la formation des bulles, accompagnée par une baisse de la température du produit, de la teneur en eau, et donc une augmentation de la température de la transition vitreuse  $T_g$ . C'est un phénomène complexe qui englobe la dynamique de nucléation, de croissance, de coalescence et de rupture des bulles dans une matrice viscoélastique, puis la solidification, voire l'effondrement à proximité de  $T_g$ . A l'heure actuelle, aucun modèle déterministe n'est disponible pour décrire ces phénomènes conjointement. En outre, un modèle déterministe serait trop complexe, et ne pourrait être couplé avec le modèle mécanistique du logiciel de simulation d'extrusion bi-vis (Ludovic®), afin de prédire directement la structure cellulaire des mousses amylacées.

L'objectif de ce travail est d'élaborer un modèle phénoménologique d'expansion afin de pouvoir le coupler avec Ludovic®. A partir de résultats expérimentaux de la bibliographie qui couvrent un large domaine de conditions thermomécaniques (environ 400 points expérimentaux), une carte conceptuelle qui décrit des relations d'influence entre les variables d'entrée et de sortie du modèle d'expansion a été construite. Elle prend en compte les phénomènes de nucléation, croissance de bulles, coalescence, rupture et fixation. Les variables d'entrée, telles que la température  $T$ , l'énergie mécanique spécifique  $SME$  et la viscosité en cisaillement  $\eta$  à la sortie de la filière, peuvent être calculées par Ludovic®. Les autres sont la teneur en eau  $MC$ , la géométrie de la filière  $h/h_d$  et le module de stockage  $E'(T > T_g)$ . Cette dernière propriété représente la viscosité élongationnelle des amidons pour une teneur en amylose variable (0-70%). Les variables de sortie sont la macrostructure et la structure cellulaire des mousses solides. La macrostructure est décrite par les indices d'expansion et l'anisotropie. La finesse de la cellule  $F$ , calculée à partir de la taille moyenne des cellules  $MCS$  et de l'épaisseur moyenne de la paroi cellulaire  $MWT$ , définit la structure cellulaire. Par la suite, une expression mathématique générale du modèle est proposée pour  $VEI$  et  $SEI$ , les indices d'expansion volumétrique et radiale, respectivement:  $VEI$  et  $SEI = \alpha (\eta / \eta_0)^n$  avec  $\alpha$  et  $n$  dépendant de  $T$ ,  $MC$ ,  $SME$ ,  $h/h_d$  et  $E'$ . A partir des valeurs connues de  $VEI$  et  $SEI$ , nous avons pu prédire l'anisotropie d'expansion ( $AF$ ), par la relation  $AF = VEI / SEI^{3/2}$ . Un bon accord entre les résultats de simulation et ceux expérimentaux est obtenu. En outre, nous avons montré que la finesse de cellule  $F$  peut être modélisée en fonction de l'anisotropie  $AF$ .